

A bright millisecond radio burst of extragalactic origin

D. R. Lorimer,^{1,2*} M. Bailes,³ M. A. McLaughlin,^{1,2}
D. J. Narkevic,¹ F. Crawford⁴

¹Department of Physics, West Virginia University, P.O. Box 6315, WV 26506 USA

²National Radio Astronomy Observatory, P.O. Box 2, Green Bank, WV 24944

³Centre for Astrophysics and Supercomputing, Swinburne University of Technology,
P.O. Box 218, Hawthorn, Vic, 3122, Australia

⁴Department of Physics and Astronomy, Franklin and Marshall College, Lancaster, PA 17604 USA

*To whom correspondence should be addressed; E-mail: Duncan.Lorimer@mail.wvu.edu.

Accepted for publication in the journal Science

Pulsar surveys offer one of the few opportunities to monitor even a small fraction ($\sim 10^{-5}$) of the radio sky for impulsive burst-like events with millisecond durations. In analysis of archival survey data, we have discovered a 30-Jy dispersed burst of duration < 5 ms located three degrees from the Small Magellanic Cloud. The burst properties argue against a physical association with our Galaxy or the Small Magellanic Cloud. Current models for the free electron content in the Universe imply the burst is < 1 Gpc distant. No further bursts are seen in 90-hr of additional observations, implying that it was a singular event such as a supernova or coalescence of relativistic objects. Hundreds of similar events could occur every day and act as insightful cosmological probes.

Transient radio sources are difficult to detect, but can potentially provide insights into a wide variety of astrophysical phenomena (*I*). Of particular interest is the detection of short-duration (\leq few ms) radio bursts that may be produced by exotic events at cosmological distances such

as merging neutron stars (2) or evaporating black holes (3). Pulsar surveys are currently one of the only records of the sky with good sensitivity to radio bursts, and the necessary temporal and spectral resolution required to unambiguously discriminate between short-duration astrophysical bursts and terrestrial interference. Indeed, they have recently been successfully mined to detect a new Galactic population of transients associated with rotating neutron stars (4). The burst we report here, however, has a significantly higher inferred energy output than this class and is not observed to repeat. This burst, therefore, represents an entirely new phenomenon.

The burst was discovered during a search of archival data from a 1.4-GHz survey of the Magellanic Clouds (5) using the multibeam receiver on the 64-m Parkes radio telescope (6) in Australia. The survey consisted of 209 telescope pointings, each lasting 2.3 hr. During each pointing, the multibeam receiver collected independent signals from 13 different positions (beams) on the sky. The data from each beam were one-bit sampled every millisecond over 96 frequency channels spanning a 288-MHz wide band. Radio signals from all celestial sources propagate through a cold ionized plasma of free electrons before reaching the telescope. The plasma, which exists within our Galaxy and in extragalactic space, has a refractive index which is frequency dependent. As a result, any radio signal of astrophysical origin should exhibit a quadratic shift in their arrival time as a function of frequency, with the only unknown being the integrated column density of free electrons along the line of sight, known as the dispersion measure (DM). Full details of the data reduction procedure to account for this effect, and to search for individual dispersed bursts, are given in the supporting online material. In brief, for each beam, the effects of interstellar dispersion were minimized for 183 trial DMs in the range 0–500 cm^{-3} pc. The data were then searched for individual pulses with signal-to-noise ratios (S/N) greater than four using a matched filtering technique (7) optimized for pulse widths in the range 1 ms–1 s. The burst was detected in data taken on 2001 August 24 with $\text{DM} = 375 \text{ cm}^{-3}$ pc contemporaneously in three neighboring beams (Fig. 1), and is located approximately three

degrees south of the center of the Small Magellanic Cloud (SMC).

The pulse exhibits the characteristic quadratic delay as a function of radio frequency (Fig. 2) expected from dispersion by a cold ionized plasma along the line of sight (l_0). Also evident is a significant evolution of pulse width across the observing frequency band. The behavior we observe, where the pulse width W scales with frequency f as $W \propto f^{-4.8 \pm 0.4}$, is consistent with pulse-width evolution due to interstellar scattering with a Kolmogorov power law ($W \propto f^{-4}$, 11). The filterbank system has finite frequency and time resolution, which effectively sets an upper limit to the intrinsic pulse width $W_{\text{int}} = 5$ ms. We represent this below by the parameter $W_5 = W_{\text{int}}/5$ ms. Note that it is entirely possible that the intrinsic width could be much smaller than observed (i.e. $W_5 \ll 1$) and the combination of intergalactic scattering and our instrumentation smear it to the resolution we see in Fig. 2.

We can estimate the flux density of the radio burst in two ways. For the strongest detection, which saturated the single-bit digitizer in the observing system, we make use of the fact that the integrating circuit that sets the mean levels and thresholds is analog. When exposed to a source of strength comparable to the system equivalent flux density, an absorption feature in the profile is induced that can be used to estimate the integrated burst energy. For a 5-ms burst we estimate the peak flux to be 40 Jy (1 Jy $\equiv 10^{-26}$ W m $^{-2}$ Hz $^{-1}$). Using the detections from the neighboring beam positions, and the measured response of the multibeam system as a function of off-axis position (θ), we determined the peak flux density to be at least 20 Jy. We therefore adopt a burst flux of 30 ± 10 Jy, which is consistent with our measurements, for the remaining discussion. Although we have only a limited information on the flux density spectrum, as seen in Fig. 2, the pulse intensity increases at the lowest frequencies of our observing band. This implies that the flux density S scales with observing frequency f as $S \propto f^{-4}$.

It is very difficult to attribute this burst to anything but a celestial source. The frequency dispersion and pulse-width frequency evolution argue for a cosmic origin. It is very unlikely

that a swept-frequency transmitter could mimic both the cold plasma dispersion law to high accuracy (see Fig. 2), and have a scattering relation consistent with the Kolmogorov power law. Furthermore, terrestrial interference often repeats, and this was the only significantly dispersed burst detected with $S/N > 10$ in the analysis of data from almost 3000 separate positions. Sources with flux densities greater than about 1 Jy are typically detected in multiple receivers of the multibeam system. While this is true for both terrestrial and astrophysical sources, the telescope had an elevation of $\sim 60^\circ$ at the time of the observation, making it virtually impossible for ground-based transmitters to be responsible for a source that was only detected in three adjacent beams of the pointing.

We have extensively searched for subsequent radio pulses from this enigmatic source. Including the original detection, there were a total of 27 beams in the survey data which pointed within 30 arcmin of the nominal burst position. These observations, which total 50 hr, were carried out between 2001 June 19 and July 24 and show no significant bursts. In April 2007 we carried out 40 hr of follow-up observations with the Parkes telescope at 1.4 GHz with similar sensitivity to the original observation. No bursts were found in a search over the DM range 0–500 cm^{-3} pc. These dedicated follow-up observations provide the best sensitivity and imply that the event rate must be less than 0.025 hr^{-1} for bursts with $S/N > 6$, i.e. a 1.4-GHz peak flux density greater than 300 mJy. The data were also searched for periodic radio signals using standard techniques (10) with null results.

The Galactic latitude ($b = -41.8^\circ$) and high DM of the burst make it highly improbable for the source to be located within our Galaxy. The most recent model of the Galactic distribution of free electrons (12) predicts a DM contribution of only 25 cm^{-3} pc for this line of sight. In fact, of over 1700 pulsars currently known, none of the 730 with $|b| > 3.5^\circ$ has $\text{DM} > 375 \text{ cm}^{-3}$ pc. The DM is also far higher than any of the 18 known radio pulsars in the Magellanic clouds (5), the largest of which is for PSR J0131–7310 in the SMC with $\text{DM} = 205 \text{ cm}^{-3}$ pc. The other

four known radio pulsars in the SMC have DMs of 70, 76, 105 and $125 \text{ cm}^{-3} \text{ pc}$. The high DM of PSR J0131–7310 is attributed (5) to its location in an HII region (see Fig. 1). We have examined archival survey data to look for ionized structure such as $\text{H}\alpha$ filaments or HII regions which could similarly explain the anomalously large DM of the burst. No such features are apparent. The source lies three degrees south from the center of the SMC, placing it outside all known contours of radio, infrared, optical and high-energy emission from the SMC. This, and the high DM, strongly suggest that the source is well beyond the SMC, which lies $61 \pm 3 \text{ kpc}$ away (13).

No published gamma-ray burst or supernova explosion is known at this epoch or position, and no significant gamma-ray events were detected by the Third Interplanetary Network (14, 15) around the time of the radio burst. The Principal Galaxy Catalog (PGC; 16) was searched for potential hosts to the burst source. The nearest candidate (PGC 246336) is located 5 arcmin south of the nominal burst position, but the non-detection of the burst in the beam south of the brightest detection appears to rule out an association. If the putative host galaxy were similar in type to the Milky Way, the non detection in the PGC (limiting B magnitude of 18) implies a rough lower limit of $\sim 600 \text{ Mpc}$ on the distance to the source.

We can place an upper bound on the likely distance to the burst from our DM measurement. Assuming a homogeneous intergalactic medium in which all baryons are fully ionized, the intergalactic DM is expected (17, 18) to scale with redshift, z , as $\text{DM} \sim 1200z \text{ cm}^{-3} \text{ pc}$ for $z \leq 2$. Subtracting the expected contribution to the DM from our Galaxy, we infer $z = 0.3$ which corresponds to a distance of about 1 Gpc. This is likely an upper limit, since a host Galaxy and local environment could both contribute to the observed DM. Using the electron density model for our Galaxy (12) as a guide, we estimate that there is a 25% probability that the DM contribution from a putative host galaxy is $> 100 \text{ cm}^{-3} \text{ pc}$ and, hence, $z < 0.2$. Obviously the more distant the source, the more powerful it becomes as a potential cosmological probe.

The sole event, however, offers little hope of a definitive answer at this stage. To enable some indicative calculations about potential source luminosity and event rates we adopt a distance of 500 Mpc. This corresponds to $z \sim 0.12$ and a host galaxy DM of $200 \text{ cm}^{-3} \text{ pc}$. In recognition of the considerable distance uncertainty, we parameterize this as $D_{500} = D/500 \text{ Mpc}$. If this source is well beyond the local group, it would provide the first definitive limit on the ionized column density of the intra-cluster medium, which is currently poorly constrained (19).

What is the nature of the burst source? From the observed burst duration, flux density and distance, we estimate the brightness temperature and energy released to be $\sim 10^{34}(D_{500}/W_5)^2 \text{ K}$ and $\sim 10^{33}W_5D_{500}^2 \text{ J}$ respectively. These, and light-travel-time arguments which limit the source size to $< 1500 \text{ km}$, for a non-relativistic source imply a coherent emission process from a compact region. Relativistic sources with bulk velocity v are larger by a factor of either Γ (for a steady jet model) or Γ^2 (for an impulsive blast model), where the Lorentz factor $\Gamma = (1 - v^2/c^2)^{-1/2}$ and c is the speed of light.

The only two currently known radio sources capable of producing such bursts are the rotating radio transients (RRATs), thought to be produced by intermittent pulsars (4), and giant pulses from either a millisecond pulsar or young energetic pulsar. A typical pulse from a RRAT would only be detectable out to $\sim 6 \text{ kpc}$ with our observing system. Even some of the brightest giant pulses from the Crab pulsar, with peak luminosities of 4 kJy kpc^2 (20), would be observable out to $\sim 100 \text{ kpc}$ with the same system. In addition, both the RRAT bursts and giant pulses follow power-law distributions of pulse energies. The strength of this burst, which is some two orders of magnitude above our detection threshold, should have easily led to many events at lower pulse energies, either in the original survey data or follow-up observations. Hence, it appears to represent an entirely new class of radio source.

To estimate the rate of similar events in the radio sky, we note that the survey we have analyzed observed for 20 d and was sensitive to bursts of this intensity over an area of about

9 deg² (i.e. 1/4500th of the entire sky) at any given time. Assuming the bursts to be distributed isotropically over the sky, we infer a nominal rate of $\sim 4500/20 = 225$ similar events per day. Given our observing system parameters, we estimate that a 10³³-Jy radio burst would be detectable out to $z \sim 0.3$, or a distance of 1 Gpc. The corresponding cosmological rate for bursts of this energy is therefore $\sim 50 \text{ d}^{-1} \text{ Gpc}^{-3}$. Though considerably uncertain, this is somewhat higher than the corresponding estimates of other astrophysical sources, such as binary neutron star inspirals ($\sim 3 \text{ d}^{-1} \text{ Gpc}^{-3}$; 21) and gamma-ray bursts ($\sim 4 \text{ d}^{-1} \text{ Gpc}^{-3}$; 22), but well below the rate of core-collapse supernovae ($\sim 1000 \text{ d}^{-1} \text{ Gpc}^{-3}$; 23). Although the implied rate is compatible with gamma-ray bursts, the brightness temperature and radio frequency we observe for this burst are significantly higher than currently discussed mechanisms or limitations for the observation of prompt radio emission from these sources (24).

Regardless of the physical origin of this burst, we predict that existing data from other pulsar surveys with the Parkes Multibeam system (25, 26, 27, 28) should contain several similar bursts. Their discovery would permit a more reliable estimate of the overall event rate. The only other published survey for radio transients on this timescale (29) did not have sufficient sensitivity to detect similar events at the rate predicted here. At lower frequencies (~ 400 MHz) where many pulsar surveys were conducted, although the steep spectral index of the source implies an even higher flux density, the predicted scattering time (~ 2 s) would make the bursts difficult to detect over the radiometer noise. At frequencies near 100 MHz where low frequency arrays currently under construction will operate (30), the predicted scattering time would be of order several minutes, and hence be undetectable.

Perhaps the most intriguing feature of this burst is its 30-Jy strength. While this has allowed us to make a convincing case for its extraterrestrial nature, the fact that it is over 100 times our detection threshold makes its uniqueness puzzling. Often, astronomical sources have a flux distribution that would naturally lead to many burst detections of lower significance; such events

are not observed in our data. If, on the other hand, this burst was a rare standard candle, more distant sources would have such large DMs that they would be both significantly red-shifted to lower radio frequencies and outside our attempted dispersion trials. If redshifts of their host galaxies are measurable, the potential of a population of radio bursts at cosmological distances to probe the ionized intergalactic medium (31) is very exciting, especially given the construction of wide-field instruments (32) in preparation for the Square Kilometre Array (33).

References and Notes

1. J. M. Cordes, T. J. W. Lazio, M. A. McLaughlin, *New Astronomy Review* **48**, 1459 (2004).
2. B. M. S. Hansen, M. Lyutikov, *MNRAS* **322**, 695 (2001).
3. M. J. Rees, *Nature* **266**, 333 (1977).
4. M. A. McLaughlin, *et al.*, *Nature* **439**, 817 (2006).
5. R. N. Manchester, G. Fan, A. G. Lyne, V. M. Kaspi, F. Crawford, *ApJ* **649**, 235 (2006).
6. L. Staveley-Smith, *et al.*, *PASA* **13**, 243 (1996).
7. J. M. Cordes, M. A. McLaughlin, *ApJ* **596**, 1142 (2003).
8. J. E. Gaustad, P. R. McCullough, W. Rosing, D. Van Buren, *PASP* **113**, 1326 (2001).
9. S. Stanimirović, L. Staveley-Smith, J. M. Dickey, R. J. Sault, S. L. Snowden, *MNRAS* **302**, 417 (1999).
10. D. R. Lorimer, M. Kramer, *Handbook of Pulsar Astronomy* (Cambridge University Press, 2005).
11. L. C. Lee, J. R. Jokipii, *ApJ* **206**, 735 (1976).

12. J. M. Cordes, T. J. W. Lazio (2002). astro-ph/0207156.
13. R. W. Hilditch, I. D. Howarth, T. J. Harries, *MNRAS* **357**, 304 (2005).
14. K. Hurley, *et al.*, *ApJS* **164**, 124 (2006).
15. K. Hurley (2007). Private communication.
16. G. Paturel, *et al.*, *A&A* **412**, 45 (2003).
17. K. Ioka, *ApJ* **598**, L79 (2003).
18. S. Inoue, *MNRAS* **348**, 999 (2004).
19. P. R. Maloney, J. Bland-Hawthorn, *ApJ* **522**, L81 (1999).
20. J. M. Cordes, N. D. R. Bhat, T. H. Hankins, M. A. McLaughlin, J. Kern, *ApJ* **612**, 375 (2004).
21. V. Kalogera, *et al.*, *ApJ* **601**, L179 (2004).
22. D. Guetta, M. Della Valle, *ApJ* **657**, L73 (2007).
23. P. Madau, M. Della Valle, N. Panagia, *MNRAS* **297**, L17 (1998).
24. J.-P. Macquart, *ApJ* **658**, L1 (2007).
25. R. N. Manchester, *et al.*, *MNRAS* **328**, 17 (2001).
26. R. T. Edwards, M. Bailes, W. van Straten, M. C. Britton, *MNRAS* **326**, 358 (2001).
27. M. Burgay, *et al.*, *MNRAS* **368**, 283 (2006).
28. B. A. Jacoby, M. Bailes, S. M. Ord, H. S. Knight, A. W. Hotan, *ApJ* **656**, 408 (2007).

29. S. W. Amy, M. I. Large, A. E. Vaughan, *Proceedings of the Astronomical Society of Australia* **8**, 172 (1989).
30. B. W. Stappers, A. G. J. van Leeuwen, M. Kramer, D. Stinebring, J. Hessels, *Proceedings of the 363. Heraeus Seminar on Neutron Stars and Pulsars*, W. Becker, H. H. Huang, eds. (Bad Honnef, 2006), pp. 101–103. astro-ph/0701229.
31. V. L. Ginzburg, *Nature* **246**, 415 (1973).
32. S. Johnston, *et al.*, ATNF SKA Memo no. 13 (2007).
33. P. N. Wilkinson, K. I. Kellermann, R. D. Ekers, J. M. Cordes, T. J. W. Lazio, *New Astron. Rev.* **48**, 1551 (2004).
34. The Parkes radio telescope is part of the Australia Telescope, which is funded by the Commonwealth of Australia for operation as a National Facility managed by CSIRO. We thank Dick Manchester for making the archival data available to us. This research has made use of data obtained from the High Energy Astrophysics Science Archive Research Center (HEASARC), provided by NASA’s Goddard Space Flight Center. We thank Kevin Hurley for providing access to the GCN network Archive and Vlad Kondratiev, Steven Tingay, Simon Johnston, Fernando Camilo and Joss Bland-Hawthorn for useful comments on the manuscript. We acknowledge the prompt awarding of follow-up time by the ATNF Director and thank Lawrence Toomey and Peter Sullivan for observing assistance.

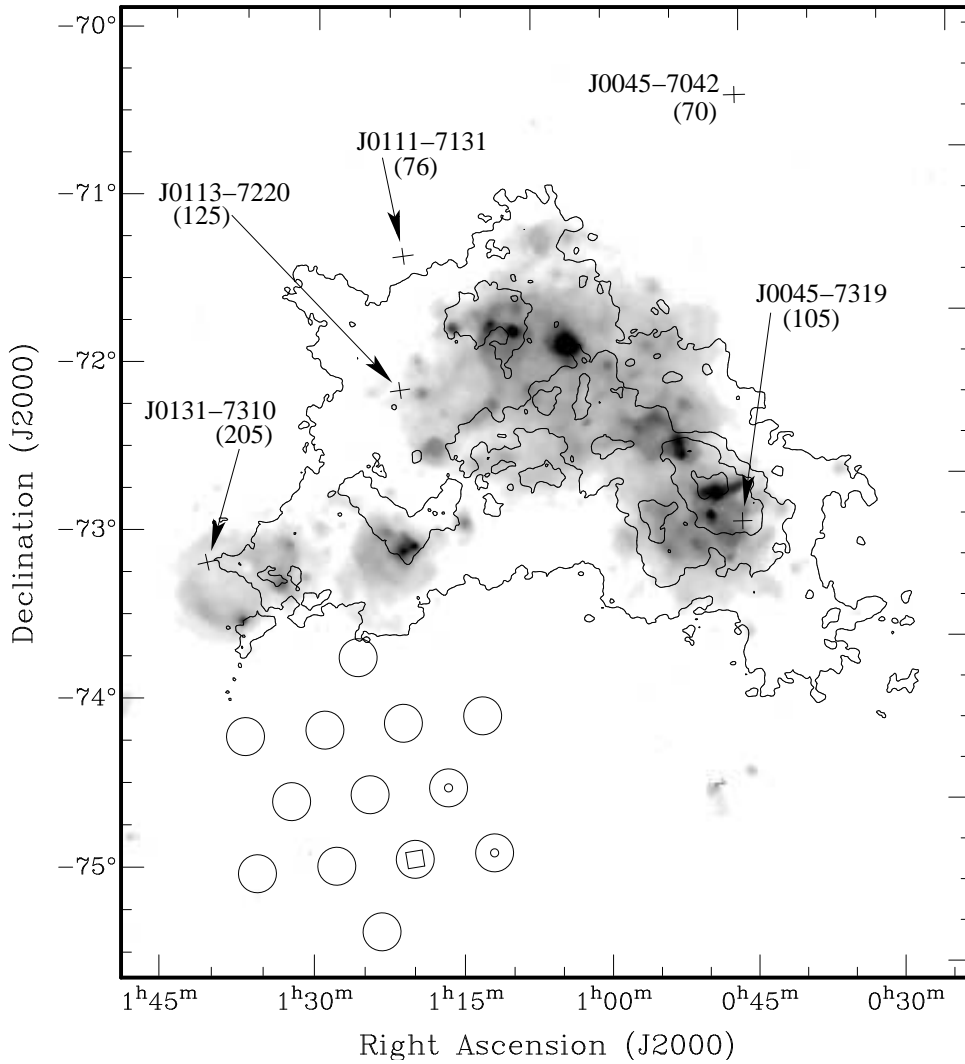


Figure 1: Multi-wavelength image of the field surrounding the burst. The gray scale and contours respectively show $H\alpha$ and HI emission associated with the SMC (8, 9). Crosses mark the positions of the five known radio pulsars in the SMC and are annotated with their names and DMs in parentheses in units of $\text{cm}^{-3} \text{ pc}$. The open circles show the positions of each of the 13 beams in the survey pointing of diameter equal to the half-power width. The strongest detection saturated the single-bit digitizers in the data acquisition system, indicating that its $S/N \gg 23$. Its location is marked with a square at right ascension $01^{\text{h}} 18^{\text{m}} 06^{\text{s}}$ and declination $-75^{\circ} 12' 19''$ (J2000 coordinates). The other two detections (with S/N s of 14 and 21) are marked with smaller circles. The saturation makes the true position difficult to localize accurately. Based on the half-power width of the multibeam system, the positional uncertainty is nominally $\pm 7'$. However, the true position is probably slightly (\sim few arcmin) north-west of this position given the non-detection of the burst in the other beams.

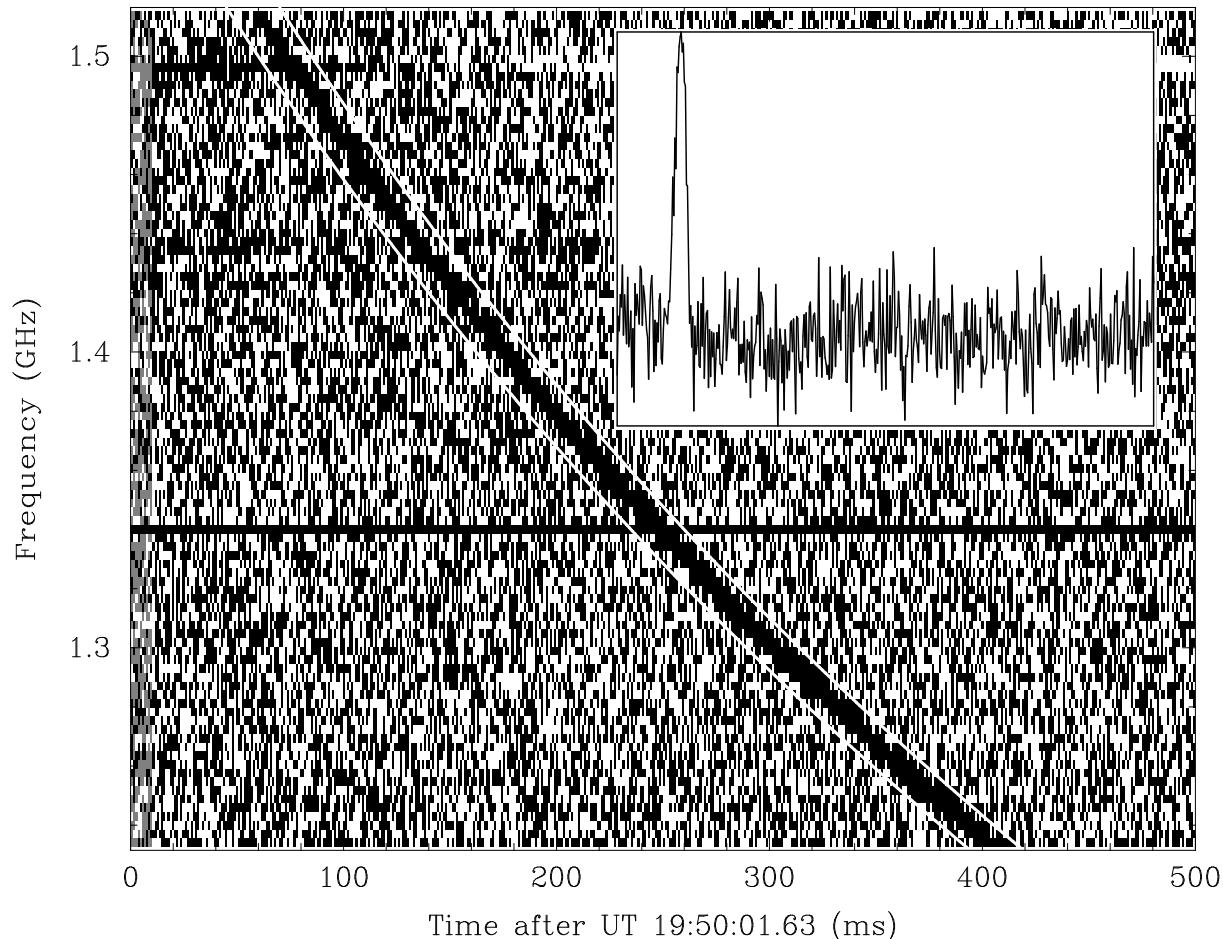


Figure 2: Frequency evolution and integrated pulse shape of the radio burst. The survey data, collected on 2001 August 24, are shown here as a two-dimensional ‘waterfall plot’ of intensity as a function of radio frequency versus time. The dispersion is clearly seen as a quadratic sweep across the frequency band, with broadening towards lower frequencies. From a measurement of the pulse delay across the receiver band using standard pulsar timing techniques, we determine the DM to be $375 \pm 1 \text{ cm}^{-3} \text{ pc}$. The two white lines separated by 15 ms that bound the pulse show the expected behavior for the cold-plasma dispersion law assuming a DM of $375 \text{ cm}^{-3} \text{ pc}$. The horizontal line at $\sim 1.34 \text{ GHz}$ is an artifact in the data caused by a malfunctioning frequency channel. This plot is for one of the offset beams in which the digitizers were not saturated. By splitting the data into four frequency sub-bands we have measured both the half-power pulse width and flux density spectrum over the observing bandwidth. Accounting for pulse broadening due to known instrumental effects, we determine a frequency scaling relationship for the observed width $W = 4.6 \text{ ms} (f/1.4 \text{ GHz})^{-4.8 \pm 0.4}$, where f is the observing frequency. A power-law fit to the mean flux densities obtained in each sub-band yields a spectral index of -4 ± 1 . Inset: the total-power signal after a dispersive delay correction assuming a DM of $375 \text{ cm}^{-3} \text{ pc}$ and a reference frequency of 1.5165 GHz . The time axis on the inner figure also spans the range 0–500 ms.

Materials and methods

We now describe the techniques used to search for isolated dispersed bursts in the survey data. In general, we follow the methodology developed and described in detail by Cordes & McLaughlin (S1). The entire survey of the Magellanic clouds (S2) amounted to 209 telescope pointings, each consisting of a 2.3-hr observation of 13 independent positions (beams) on the sky. The data for each beam were recorded as 96 frequency channels spanning the band 1.2285–1.5165 GHz sampled contiguously at 1 ms intervals. Each of the 2717 beams from the survey was processed independently using freely available software (S3) in the following sequence: interference excision, time series generation, baseline removal, single-pulse detection and diagnostic plot production.

Interference excision

To minimize the number of impulsive bursts from terrestrial sources, for each sample the sum of the 96 frequency channels was computed. For truly unbiased single-bit data, the expected sum is 48 (i.e. half zeros and half ones) with a standard deviation of $\sqrt{48} = 6.9$. Those samples which deviated from this ideal value by more than three standard deviations were flagged and not used in any subsequent analysis. This ‘clipping’ process resulted in about 5% of the entire data being discarded.

Time series generation

Electromagnetic waves propagating through an ionized plasma experience a frequency dependent delay across the observing frequency band due to the dispersive effects of the plasma. The difference in arrival times, Δt , between a pulse received at a high frequency, f_{high} , and a lower

frequency, f_{low} , is given by the cold-plasma dispersion law (S4):

$$\Delta t = 4.148808 \text{ ms} \times \left[\left(\frac{f_{\text{low}}}{\text{GHz}} \right)^{-2} - \left(\frac{f_{\text{high}}}{\text{GHz}} \right)^{-2} \right] \times \left(\frac{\text{DM}}{\text{cm}^{-3} \text{ pc}} \right), \quad (1)$$

where DM is the integrated column density of free electrons in the ionized medium. This formula was used to calculate the delays of lower frequency channels with respect to the highest frequency channel in our band. For a given DM, we can remove dispersion by summing the individual frequency channels together and appropriately delaying the lower-frequency channels with respect to the highest frequency channel. The resulting data product is known as a ‘dedispersed time series’. Since the DM of a source is a-priori unknown, this process is repeated multiple times to produce a set of time series spanning a range of DMs. In our analysis, 183 time series were produced for each beam, corresponding to the DM range 0–500 $\text{cm}^{-3} \text{ pc}$. The DM step size was chosen such that the delay introduced at a slightly incorrect trial DM was always less than one time sample. For this survey, any residual broadening of pulses in the data is always less than 1 ms.

Time series normalization

The time series produced in the previous step have an offset which reflects the system noise in the receiver. This offset may vary significantly during the integration due to receiver and background noise variations in the observing system. These effects were mitigated by dividing each time series into 8 segments. For each segment, we subtract its mean from each sample therein and compute the resulting standard deviation, σ . To ensure that the mean and standard deviation are not biased by bright individual pulses, the procedure is performed twice, with pulses detected during the first pass omitted from the mean and standard deviation calculation of the second pass.

Single-pulse detection

Individual samples are considered potentially significant if they have amplitudes $A > 4\sigma$ (S1). This simple thresholding process is most sensitive to pulses of width equal to the sampling interval (i.e. 1 ms in our case) and can be considered as an ideal matched filter to such pulses. To optimize sensitivity to broader pulses, samples are added in pairs, the standard deviation is recomputed and the 4σ threshold is again applied. This process is repeated a total of 10 times until a time resolution of 1.024 s has been reached. The absolute time index, pulse width with the highest signal-to-noise ratio (S/N; defined simply as A/σ) and the S/N itself are stored for subsequent analysis.

The standard deviation, σ , also contains useful information for calibration purposes. Using a modified form of the radiometer equation (S4), the root mean square noise fluctuations in Jy can be written as

$$\Delta S_{\text{sys}} = \frac{\beta T_{\text{sys}}}{G \sqrt{n_{\text{p}} N_{\text{add}} t_{\text{samp}} \Delta f}} = C\sigma, \quad (2)$$

where $\beta = \sqrt{\pi/2}$ is a factor accounting for losses due to 1-bit digitization, $T_{\text{sys}} \approx 30$ K is the system noise temperature in the receiver, $G \approx 0.7$ K Jy⁻¹ is the antenna gain, N_{add} is the number of times the time samples have been added in pairs, $t_{\text{samp}} = 1$ ms is data sampling interval and $\Delta f = 288$ MHz is the receiver bandwidth and C is the required scaling factor in units of Jy per standard deviation. In the flux density estimates given in the paper, we calibrated the S/N into Jy by simply multiplying them by C .

Diagnostic plotting

The search output is stored for offline visual inspection as a set of diagnostic plots. We show two examples of such plots for a detection of the known pulsar in the Large Magellanic Cloud B0529–66 (Fig. S1) and the discovery observation of the burst reported in this paper (Fig. S2).

In both cases, the dispersed pulses are clearly visible above the background noise.

Each diagnostic plot was carefully scrutinized and potentially significant events were saved for follow-up analysis in which the events were examined in the time–frequency plane as shown in Fig. 2 of the main paper. Two known pulsars B0529–66 and B0540–69 were identified as a result of this process. The only remaining signal from the survey which clearly follows the cold-plasma dispersion law was the burst reported in the paper.

References and Notes

- S1. J. M. Cordes, M. A. McLaughlin, *ApJ* **596**, 1142 (2003).
- S2. R. N. Manchester, G. Fan, A. G. Lyne, V. M. Kaspi, F. Crawford, *ApJ* **649**, 235 (2006).
- S3. D. R. Lorimer SIGPROC pulsar data analysis tools available online at <http://sigproc.sourceforge.net>.
- S4. D. R. Lorimer, M. Kramer, *Handbook of Pulsar Astronomy* (Cambridge University Press, 2005).

File: SMC017_038A1 1685 events. max S/N = 7.2. Peak DM = 101.7 cm⁻³ pc

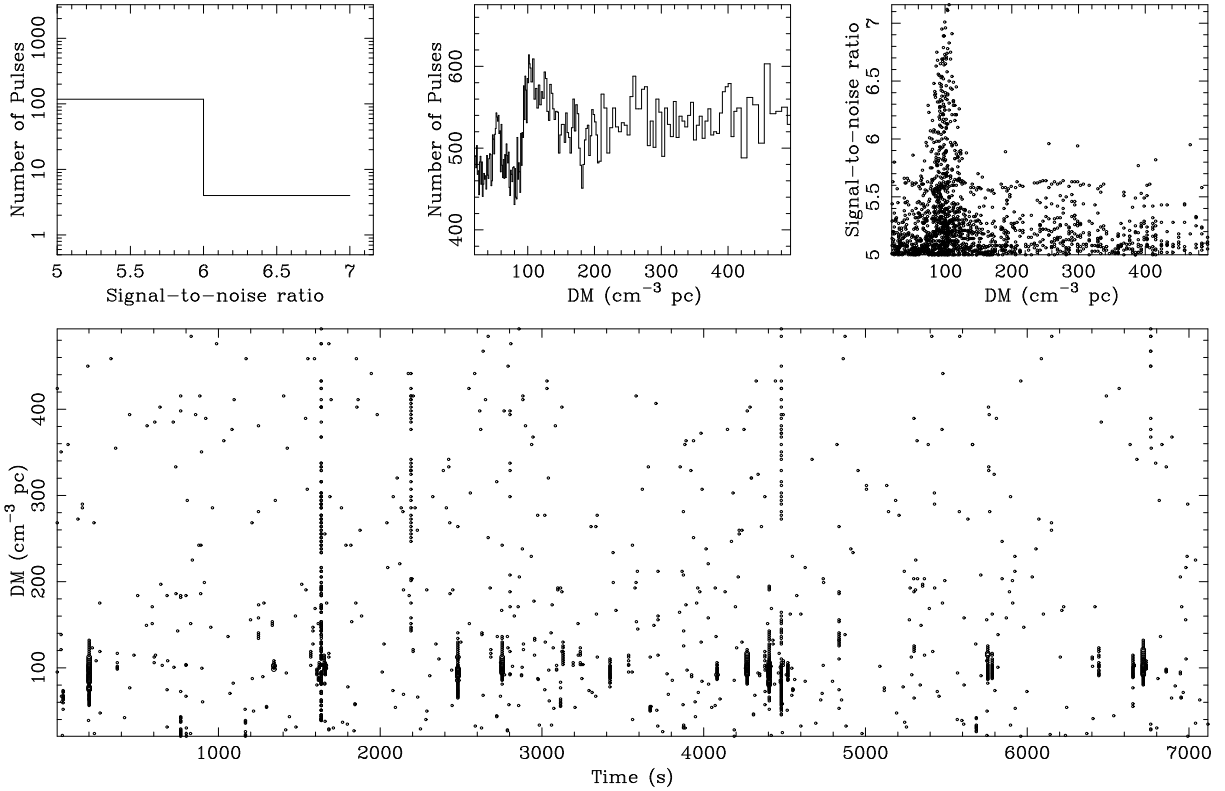


Figure S1: Single-pulse search output showing a survey detection of the known pulsar B0529–66. From left to right, the plots in the upper panel show the number of pulses detected as a function of signal-to-noise ratio (S/N), the number as a function of DM, and a scatter plot of S/N versus DM. The lower panel shows the detected pulses as a function of observation time and DM, with the size of the circles being proportional to S/N. The pulsar is clearly visible as a band of occasional pulses in this diagram, with maximum signal-to-noise at a DM of 101.7 cm⁻³ pc, and also in the S/N versus DM plot. Some locally generated interference detected across a wider range of DMs is also present.

File: SMC021_00861 1200 events. max S/N = 23.0. Peak DM = 359.1 cm⁻³ pc

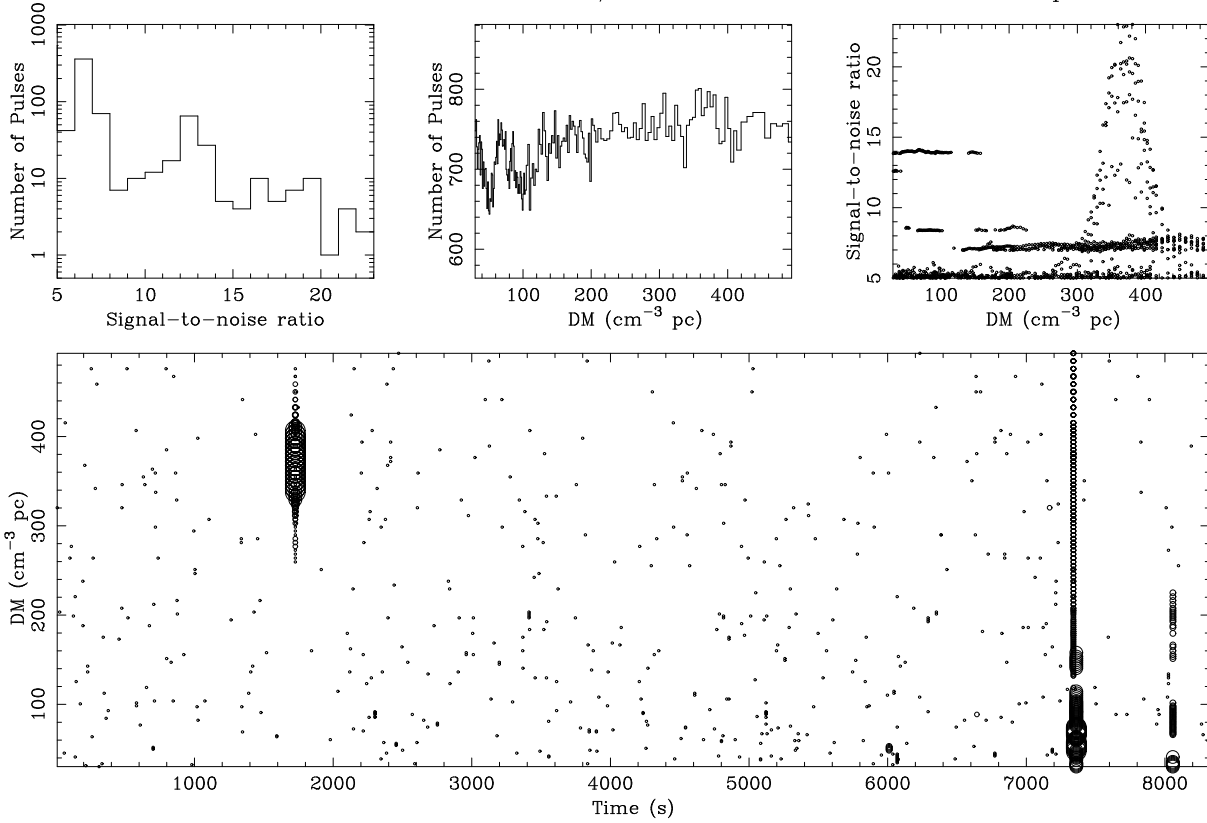


Figure S2: Single-pulse search output showing the discovery of the burst reported in this paper. See caption to Fig. S1 for details of the diagnostic plots. The burst is clearly visible in the S/N versus DM plot with a S/N of 23 and DM of 360 cm⁻³ pc (the closest trial DM to the true value determined in the paper, which was determined more precisely by an arrival-time analysis). The event is also seen in the lower panel as a highly dispersed isolated burst occurring approximately 1650 s after the start of the observation. Note also the presence of locally generated interference between 7000 and 8000 s.